Thermal Transitions in Dense Two-Colour QCD

Dale Lawlor[1,*], *Simon* Hands[2,**], *Seyong* Kim[3,***], and *Jon-Ivar* Skullerud[1,4,****]

[1]Department of Theoretical Physics; National University of Ireland, Maynooth; Maynooth; Co. Kildare; Ireland
[2]Department of Mathematical Sciences; University of Liverpool; Liverpool; L69 3BX; United Kingdom
[3]Department of Physics; Sejong University; Seoul 143–147; Republic of Korea
[4]Hamilton Institute; National University of Ireland, Maynooth; Maynooth; Co. Kildare; Ireland

Abstract. The infamous sign problem makes it impossible to probe dense (baryon density $\mu_B > 0$) QCD at temperatures near or below the deconfinement threshold. As a workaround, one can explore QCD-like theories such as two-colour QCD (QC_2D) which don't suffer from this sign problem but are qualitively similar to real QCD. Previous studies on smaller lattice volumes have investigated deconfinement and colour superfluid to normal matter transitions. In this study we look at a larger lattice volume $N_s = 24$ in an attempt to disentangle finite volume and finite temperature effects. We also fit to a larger number of diquark sources to better allow for extrapolation to zero diquark source.

1 Introduction

The objective of lattice QCD is to solve the path integral for an operator $\mathcal{O}[\Phi]$

$$\langle \mathcal{O} \rangle = \frac{1}{Z} \int \mathcal{D}[\Phi] \mathcal{O}[\Phi] e^{-S[\Phi]} \tag{1}$$

where Z is the partition function, Φ is shorthand for all the fields and S the action. S plays the role of a probability distribution function allowing us to apply Monte Carlo techniques to solve this integral. Gauge configurations U are produced with probability weight

$$e^{-S[U]} = \det M[U] e^{-S_G[U]} \tag{2}$$

where $M[U]$ is the fermion matrix. For the SU(3) gauge group with a non-zero baryon chemical potential μ_B, $\det M[U]$ can take on complex values, yielding a complex probability density. This means that dense QCD systems such as neutron stars and colour superconducting states are beyond the scope of current lattice simulation techniques. Alternatives such as reweighting, analytic continuation, the complex Langevin method, effective field theories and studies of other gauge groups are currently being employed. An overview of the first four approaches can be found in [1] with this study using the latter approach.

*e-mail: dalel487@thphys.nuim.ie, Speaker
**e-mail: simon.hands@liverpool.ac.uk
***e-mail: skim@sejong.ac.kr
****e-mail: jonivar@thphys.nuim.ie

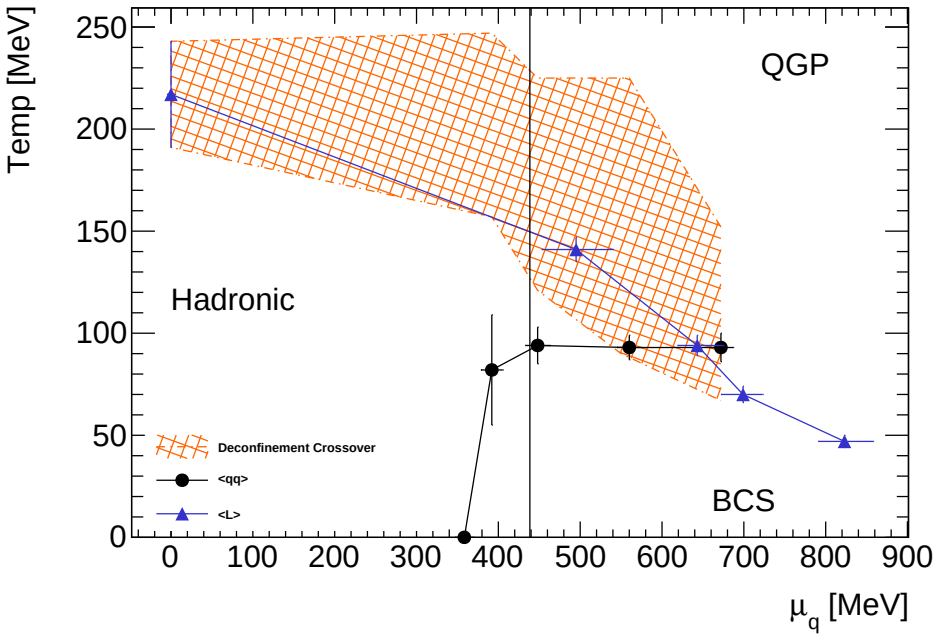

Figure 1: Phase diagram of QC$_2$D for $\frac{m_\pi}{m_\rho} = 0.80(1)$ [2]. The orange hatched area is the deconfinement crossover region, black circles correspond to the superfluid transition and the blue triangles the inflexion point of the Polyakov loop from [3].

For an SU(2) gauge group and an even number of flavours the determinant and Pfaffian are both real and non-negative for $\mu_B > 0$, thus allowing Monte Carlo techniques to be used. This two-colour version of QCD has some interesting properties, such as the role of baryons being played by bosonic diquarks. But qualitatively it is similar to three-colour QCD, sharing noticeable features such as confinement and chiral symmetry breaking.

2 Simulation details

For this simulation we are using an unimproved Wilson action with two quark flavours, with simulation parameters from table 1. The scale was set by taking the string tension $\sqrt{\sigma} = 440\,\text{MeV}$ and fitting the static quark potential to the Cornell form

$$V(r) = C + \frac{\alpha}{r} + \sigma r \tag{3}$$

at zero chemical potential [2, 3].

We look at a fixed chemical potential $\mu = 443\,\text{MeV}$ and conduct a temperature sweep. These lattice parameters were previously used for a chemical potential scan on a spatial extent of $N_s = 12$ in [4] and both temperature and chemical potential scans on a spatial extent of $N_s = 16$ in [5]. The code used for this simulation was first used in [6] and the version used for this run can be found here [7] on Zenodo.

At low temperatures we expect to find a colour superfluid phase. As the temperature increases we then expect to see a dense hadronic phase, akin to neutron stars. Beyond that we expect to undergo crossover transition to the deconfined quark-gluon plasma.

Parameter	Value
β	1.9
κ	0.1680
a (fm)	0.178(6) fm
a (GeV^{-1})	0.9 GeV^{-1}
$a\mu$	0.400
μ (MeV)	443 MeV
am_π	0.645(8)
m_π (MeV)	717(25) MeV
m_π/m_ρ	0.805(9)
N_s	24

Table 1: Configurations were generated using the above parameters for a coarse lattice as described in [4].

The temperature is given by

$$T = \frac{1}{a_\tau N_\tau} \tag{4}$$

There are two methods of controlling the temperature. By changing the lattice spacing in the temporal extent a_τ it is possible to continuously vary the temperature. However this requires setting the scale for every value of a_τ which is time and resource intensive. Instead we vary the number of sites along the time direction and use a fixed a_τ. This allows us to complete a temperature scan without setting the scale for each temperature, but at the cost of only being able to look at a discrete set of temperatures. Temperatures were scanned at N_τ = 3–20, giving temperatures in the range 55 MeV–365 MeV. As is standard practice we take the largest time extent where $N_\tau > N_s$ to be"zero-temperature", thus use the $N_\tau = 20$ value of an observable for zero temperature subtraction.

At non-zero baryon density, the fermion matrix acquires a non-zero density of very small eigenvalues, slowing down the computation significantly. Introducing a diquark source j lifts these eigenvalues, with "physical" results recovered by an extrapolation of j to zero as seen in figure 2a. Whereas previous studies have used either two or three diquark sources, this is the first time we have done a full temperature scan with four sources and have a full temperature scan with $aj = 0.010$.

3 Results

3.1 Diquark Condensate

The observables being measured are described in [6], but as a recap we'll be looking at the diquark condensate

$$\langle qq \rangle = \frac{\kappa}{2} \langle \bar{\psi}_1 C\gamma_5\tau_2 \bar{\psi}_2^{tr} - \psi_2^{tr} C\gamma_5\tau_2 \psi_1 \rangle \tag{5}$$

where C is the charge conjugation matrix. The index of the ψ term denotes flavour. This is the order parameter for the superfluid phase transition (predicted to be a second order transition).

Figure 2a shows the diquark condensate as a function of the diquark source for various temperatures. The fit $\langle qq \rangle = A + Bj^\alpha$ was used, with the y-intercept A being used as the $j = 0$ value of the diquark condensate. This fit has previously been used in [3, 5, 8] on $N_s = 12$ and $N_s = 16$ lattices using the lattice parameters from this simulation and with a finer lattice

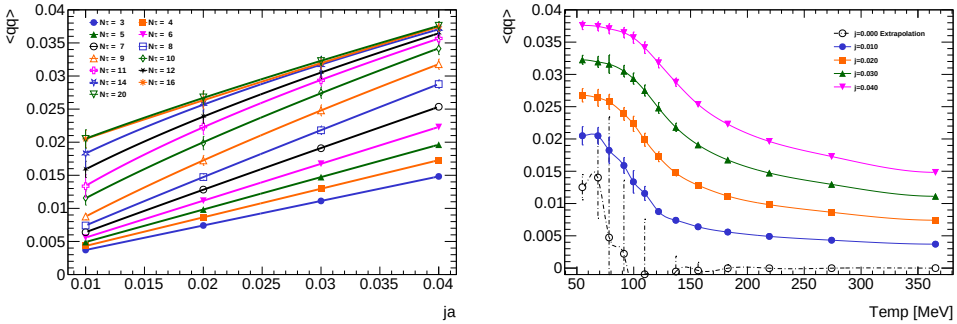

(a) Unrenormalised diquark condensate vs Diquark source.

(b) Unrenormalised diquark condensate vs Temperature.

Figure 2: Unrenormalised diquark condensate $\langle qq \rangle$ as a function of diquark source j and temperature T. We extrapolated j to zero in figure 2a to obtain the hollow points in figure 2b.

spacing $a = 0.138(6)$ fm. The $aj = 0.01$ values and the larger lattice volume have given us much improved control of the $j = 0$ extrapolation. For low and high temperatures $\langle qq \rangle$ was found to be linear in j. But around the superfluid phase transition the fit is non-linear, with the exponent reaching its minimum around the transition.

Figure 2b shows the diquark condensate as a function of temperature for various diquark sources. The hollow points correspond to the zero diquark extrapolation. We used a cubic spline for the interpolation. A linear fit of the inflexion points of the three lowest diquark sources suggests the superfluid phase transition occurs around $T \sim 84$ MeV, significantly lower than the deconfinement crossover. This indicates that the superfluid phase transition is indeed distinct from the deconfinement crossover as seen in figure 1. However an improved action and more data are required to nail down the transition temperature more precisely, in addition to an error analysis to give proper bounds on the transition temperature.

3.2 Thermodynamics

We are also interested in thermodynamic observables such as the quark number density n_q, the quark energy ε_q and the trace anomaly

$$T_{\mu\mu} = \varepsilon - 3P \tag{6}$$

We evaluated the pressure and energy density the using derivative the method, with the Karsch coefficients calculated in [3]. These results are qualitatively consistent with recent results from [9, 10]. The energy density exhibits similar behaviour. The dip in the density in figure 3a is in the same region as the superfluid phase transition. This is remarkable as $\frac{n_q}{n_{SB}}$ is not an order parameter for the phase transition.

The trace anomaly itself is smaller than expected. Also interesting is how the quark and gluon contributions nearly cancel each other out at most temperatures. This may be due to the choice of regularisation. The trace anomaly is constant and consistently zero up until $T \sim 150$ MeV, suggesting that we are in a conformal régime. Is this a sign of a second transition from conformal to non-conformal physics?

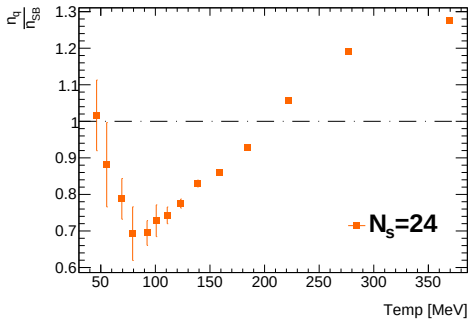

(a) Quark number density normalised by the non-interacting number density.

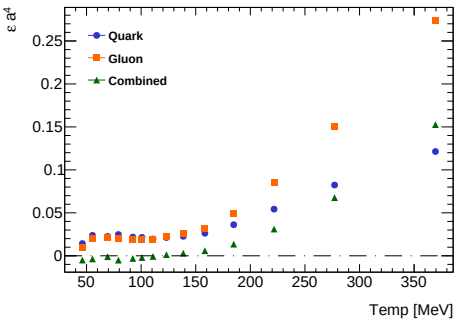

(b) Unrenormalised energy density.

Figure 3: Quark number density. These result are compatible with previous results on a smaller volume in [2].

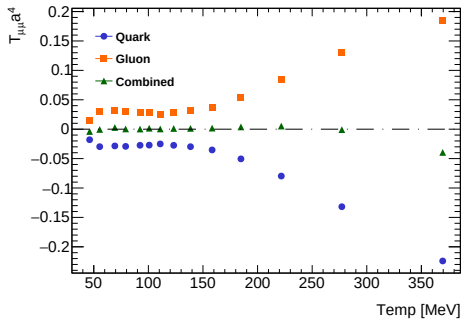

(a) Trace anomaly.

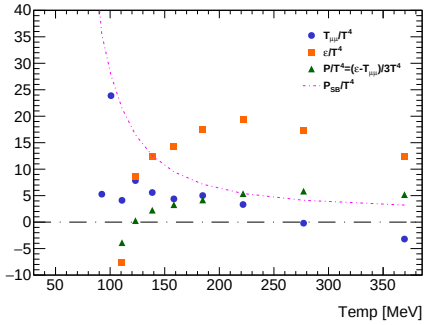

(b) Dimensionless thermodynamic observables.

Figure 4: Thermodynamic observables.

3.3 Chiral and Deconfinement Transition

Another quantity of interest is the Polyakov loop expectation value, which is the order parameter for the deconfinement crossover in pure gauge theory. The Polyakov loop was renormalised using the procedure described in [11] with the renormalisation constants previously calculated on a smaller volume in [3]. The Polyakov loop renormalisation is temperature dependent, unlike that of the diquark condensate.

$$L_R(T,\mu) = Z_L^{N_\tau} L_0\left(\frac{1}{a_\tau N_\tau}, \mu\right) \tag{7}$$

We consider two renormalisation schemes to determine Z_L

Scheme A: $L_R(N_\tau = 4, \mu = 0) = 0.5 \quad \Rightarrow Z_L = 1.37495$
Scheme B: $L_R(N_\tau = 4, \mu = 0) = 1.0 \quad \Rightarrow Z_L = 1.15619$

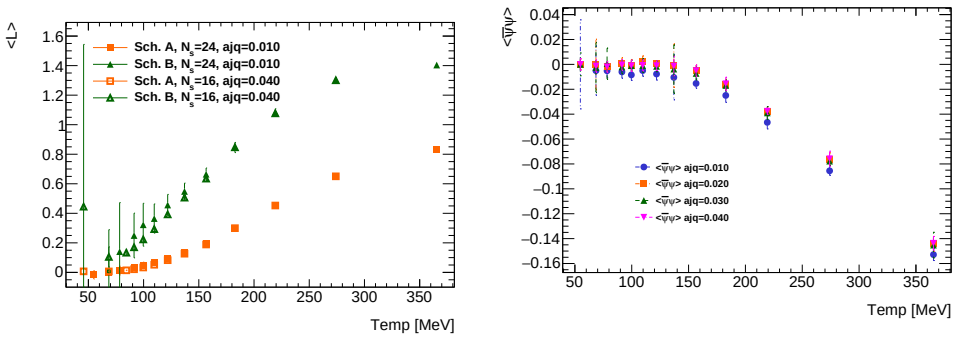

(a) Renormalised Polyakov loop

(b) Subtracted but unrenormalised chiral condensate

Figure 5: Bosonic observables

The chiral condensate with Wilson fermions has both multiplicative and additive renormalisations. The additive and multiplicative renormalisations are a constant shift and constant factor respectively. Figure 5b has undergone additive renormalisation by subtracting the zero temperature value of $\langle qq \rangle$, but multiplicative renormalisation has not been carried out. This can be done using the proceedure found in [12–14] but would merely amount to an overall rescaling of the data in figure 5b. The change in behaviour from constant to decreasing at $T \sim 150\,\mathrm{MeV}$ suggests that the crossover coincides with the deconfinement crossover, not the superfluid transition.

4 Outlook

The larger lattice volume has shown us that finite volume errors are small for these parameters. The superfluid phase transition and deconfinement crossover are distinct. Further investigation is needed into the unexpectedly small trace anomaly. Work is underway to implement a Symanzik improved fermion action. We have also started tuning for a finer lattice with lighter quarks. Combined with the improved action these "light-fine" quarks will give us better control over errors in addition to providing more physically realistic measurements.

Acknowledgements

D. Lawlor would like to acknowledge support from the National University of Ireland, Maynooth's John and Pat Hume Scholarship.

The authors wish to acknowledge the Irish Centre for High-End Computing (ICHEC) for the provision of computational facilities and support.

This work was performed using the DiRAC Data Intensive service at Leicester, operated by the University of Leicester IT Services, which forms part of the STFC DiRAC HPC Facility (www.dirac.ac.uk). The equipment was funded by BEIS capital funding via STFC capital grant ST/K000373/1 and ST/R002363/1 and STFC DiRAC Operations grant ST/R001014/1. DiRAC is part of the National e-Infrastructure.

References

[1] J.N. Guenther, *Overview of the QCD phase diagram: Recent progress from the lattice* (2021), 2010.15503
[2] *Phase transitions in dense 2-colour QCD*, Vol. LATTICE2013 (2014), 1311.1367
[3] S. Cotter, P. Giudice, S. Hands, J.I. Skullerud, Phys. Rev. D **87**, 034507 (2013), 1210.4496
[4] S. Hands, S. Kim, J.I. Skullerud, Phys. Rev. D **81**, 091502 (2010), 1001.1682
[5] T. Boz, S. Cotter, L. Fister, D. Mehta, J.I. Skullerud, Eur. Phys. J. A **49**, 87 (2013), 1303.3223
[6] S. Hands, S. Kim, J.I. Skullerud, Eur. Phys. J. C **48**, 193 (2006), hep-lat/0604004
[7] S. Hands, S. Kim, D. Lawlor, J.I. Skullerud, *su2hmc* (2022), A hybrid monte carlo algorithm for SU(2) wilson fermions, https://doi.org/10.5281/zenodo.7164407
[8] T. Boz, P. Giudice, S. Hands, J.I. Skullerud, Phys. Rev. D **101**, 074506 (2020), 1912.10975
[9] K. Iida, E. Itou (2022), 2207.01253
[10] Y. Fujimoto, K. Fukushima, L.D. McLerran, M. Praszalowicz (2022), 2207.06753
[11] S. Borsanyi, Y. Delgado, S. Durr, Z. Fodor, S.D. Katz, S. Krieg, T. Lippert, D. Nogradi, K.K. Szabo, Phys. Lett. B **713**, 342 (2012), 1204.4089
[12] G. Aarts, C. Allton, J. Glesaaen, S. Hands, B. Jäger, K. Seyong, M.P. Lombardo, A. Nikolaev, S. Ryan, J.I. Skullerud et al., Phys. Rev. D **105**, 034504 (2022), 2007.04188
[13] L. Giusti, F. Rapuano, M. Talevi, A. Vladikas, Nucl. Phys. B **538**, 249 (1999), hep-lat/9807014
[14] S. Borsanyi, S. Durr, Z. Fodor, C. Hoelbling, S.D. Katz, S. Krieg, D. Nogradi, K.K. Szabo, B.C. Toth, N. Trombitas, JHEP **08**, 126 (2012), 1205.0440